

LETTER TO THE EDITOR

What does (not) drive the variation of the low-mass end of the stellar initial mass function of early-type galaxies

MUSE Paintbox II

C. E. Barbosa^{1,*}, C. Spiniello^{2,3}, M. Arnaboldi⁴, L. Coccato⁴, M. Hilker⁴, and T. Richtler⁵

¹ Universidade de São Paulo, IAG, Departamento de Astronomia, Rua do Matão 1226, São Paulo, SP, Brazil

² Department of Physics, University of Oxford, Denys Wilkinson Building, Keble Road, Oxford OX1 3RH, UK

³ INAF, Osservatorio Astronomico di Capodimonte, Via Moiariello 16, 80131, Naples, Italy

⁴ European Southern Observatory, Karl-Schwarzschild-Straße 2, 85748, Garching, Germany

⁵ Departamento de Astronomia, Universidad de Concepción, Concepción, Chile

Received October 30, 2020; Accepted December 1, 2020

ABSTRACT

Context. The stellar initial mass function (IMF) seems to be variable and not universal, as argued in the literature in the last three decades. Several relations among the low-mass end of the IMF slope and other stellar population, photometrical or kinematical parameters of massive early-type galaxies (ETGs) have been proposed, but a consolidated agreement on a factual cause of the observed variations has not been reached yet.

Aims. We investigate the relations between the IMF and other stellar population parameters in NGC 3311, the central galaxy of the Hydra I cluster. NGC 3311 is a unique laboratory, characterized by old and metal-rich stars, like other massive ETGs for which the IMF slope has been measured to be bottom-heavy (i.e. dwarf-rich), but has unusual stellar velocity dispersion and $[\alpha/\text{Fe}]$ profiles, both increasing with radius.

Methods. We use the spatially resolved stellar population parameters (age, total metallicity, $[\alpha/\text{Fe}]$) derived in a companion paper (Barbosa et al. 2020) from Bayesian full-spectrum fitting of high signal-to-noise MUSE observations to compare the IMF slope in the central part of NGC 3311 ($R \lesssim 16$ kpc) against other stellar parameters, with the goal of assessing their relations/dependencies.

Results. For NGC 3311, we unambiguously invalidate the previously observed direct correlation between the IMF slope and the local stellar velocity dispersion, confirming some doubts already raised in the literature. This relation may arise as a spatial coincidence only, between the region with the largest stellar velocity dispersion value, with that where the oldest, *in situ* population is found and dominates the light. We also show robust evidence that the proposed IMF-metallicity relation is contaminated by the degeneracy between these two parameters. We do confirm that the stellar content in the innermost region of NGC 3311 follows a bottom-heavy IMF, in line with other literature results. The tightest correlations we found are those between stellar age and IMF and between galactocentric radius and IMF.

Conclusions. The variation of the IMF at its low-mass end is not due to kinematical, dynamical, or global properties in NGC 3311. We speculate instead that the IMF might be dwarf-dominated in the "red-nuggets" formed through a very short and intense star formation episode at high redshifts ($z > 2$), when the universe was denser and richer in gas, and that then ended up being the central cores of today giant ellipticals.

Key words. Galaxies: clusters: individual: Hydra I – Galaxies: individual: NGC 3311 – Galaxies: elliptical and lenticular, cD – Galaxies: kinematics and dynamics – Galaxies: structure – Galaxies: stellar content

1. Introduction

The IMF is the distribution of stars per unit of mass formed in a volume of space within a single star-formation event. Since the mass of a star determines its subsequent evolutionary path, the IMF influences all the observable properties of a stellar system. In addition, the IMF slope at the low-mass end modifies the stellar mass-to-light ratio value in any galaxy. In fact, low-mass stars account for more than half of the mass budget while they contribute very little to the integrated luminosity of a galaxy dominated by an old stellar population (see, e.g., Fig. 2 in Conroy & van Dokkum 2012a). This makes the characterization of the low-mass IMF slope from integrated light a challenging task, but crucial to assess the relative contribution of stars and dark mat-

ter, and to understand their relative distribution in the baryon-dominated inner galaxy regions.

In the last decade, a large number of studies reported that the low-mass end of the IMF slope in massive ETGs is bottom-heavier (i.e. dwarf-richer) in relation to the IMF inferred in the Milky Way (MW), as indicated by a variety of methods, such as stellar populations, gravitational lensing and dynamics (see Cenarro et al. 2003; van Dokkum & Conroy 2010; Treu et al. 2010; Conroy & van Dokkum 2012b; Spiniello et al. 2012, 2014; Cappellari et al. 2012; La Barbera et al. 2013, 2017). However, a general consensus on which physical quantity is really responsible for the non-universality of the IMF is far from being reached. The stellar velocity dispersion (Cappellari et al. 2012; Spiniello et al. 2014), the total mass density (Spiniello et al. 2015), the metallicity (Martín-Navarro et al. 2015c), the magnesium abun-

* Corresponding author: carlos.barbosa@usp.br.

dance (La Barbera et al. 2017), the age and the α -element abundance (McDermid et al. 2014) have been investigated so far.

More recently, spatially resolved studies have found that the bottom-heavy IMF is concentrated in the innermost region of galaxies (Martín-Navarro et al. 2015a; van Dokkum et al. 2017; Sarzi et al. 2018; Parikh et al. 2018; Vaughan et al. 2018; La Barbera et al. 2019), indicating that also local properties, not only global, may drive variation in the low-mass end of the IMF. These findings are particularly interesting in the context of the two-phase formation scenario (Naab et al. 2009; Oser et al. 2010; Hilz et al. 2012; Rodríguez-Gomez et al. 2016; Pulsoni et al. 2020), as the center is where the *in situ* population, formed during the first phase of the mass assembly dominates the light.

The majority of massive ETGs shows mostly flat or falling stellar velocity dispersion (σ_*) profiles (Fisher et al. 1995; Sembach & Tonry 1996; Carter et al. 1999; Brough et al. 2007; Emsellem et al. 2014). Consequently, the IMF has always been measured to be bottom-heavy in the region where the σ_* profile had the central peak. The same holds for the $[\alpha/\text{Fe}]$ abundance, which is often larger in the center than in the outer regions. Thus it has not been possible until now to assess independently whether the spatial variation of the low-mass end of the IMF is driven by the kinematics (i.e. the IMF is dwarf-rich wherever σ_* is high), the stellar populations (i.e. the IMF is dwarf-rich when the metallicity/ $[\alpha/\text{Fe}]$ is super solar) or rather by other mechanisms linked to the intense, early star formation (i.e. the IMF is dwarf-rich in the innermost region, where the *in situ* stars dominate, despite of the local kinematics).

In this context, NGC 3311, the central galaxy of the Hydra I cluster, is a perfect “laboratory” to disentangle between these scenarios, having both a σ_* and a $[\alpha/\text{Fe}]$ profile rising with increasing galactocentric distances¹, while the total metallicity is instead higher in the center (Barbosa et al. 2016, hereafter B16). The very peculiar profiles in NGC 3311 are the results of the presence of multiple components with distinct kinematics and stellar populations, as we show in detail in the companion paper MUSE Paintbox I (Barbosa et al. 2020, hereafter B20). There we performed a fully Bayesian, full-spectral fitting analysis on high signal-to-noise MUSE spectra and obtained accurate spatially resolved measurements of light-weighted age, metallicity ($[Z/\text{H}]$), α -element abundance ($[\alpha/\text{Fe}]$) and IMF slope (Γ_b). We refer the reader to B20 for more details about the stellar population modeling. Here we focus mainly on the low mass-end of the IMF slope and its possible correlations with the other kinematical and stellar population parameters. We note that the spatially resolved stellar population properties of NGC 3311 cover a range of metallicities, $[\alpha/\text{Fe}]$ abundances and σ_* that would allow us to observe IMF gradients and correlations, assuming the IMF depends on these parameters, in line with previous studies.

2. What drives the IMF variations?

In B20, we use the E-MILES (Vazdekis et al. 2016) stellar population (SP) models with a “bimodal” IMF (Vazdekis et al. 1996), which is obtained by changing the high-mass end ($M \gtrsim 0.6M_\odot$) power-law slope (Γ_b). The IMF is then normalized to $1M_\odot$, as more massive stars are already dead in old stellar populations, hence a change in the Γ_b slope can be interpreted as a change in the ratio between stars with masses above and below $0.6M_\odot$. In practice, we are constraining the “present-day” mass function between 0.1 and 1 solar masses.

¹ We note that few other massive galaxies with rising σ_* profiles exist, see e.g. Veale et al. (2017).

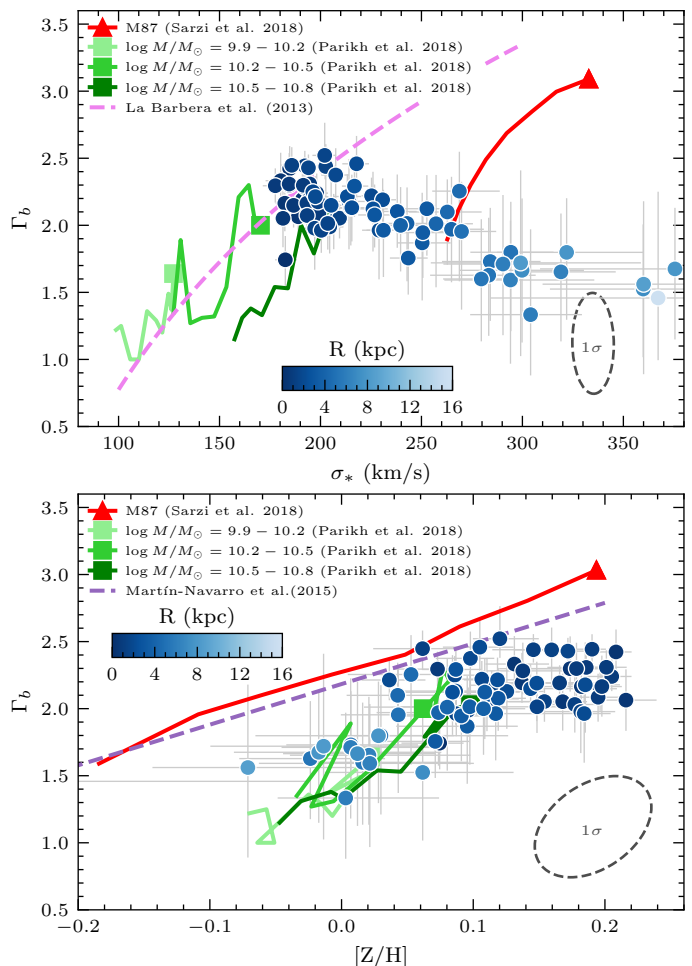


Fig. 1. IMF slope (Γ_b) versus stellar velocity dispersion (σ_* , upper panel), and total metallicity ($[Z/\text{H}]$, bottom panel). Blue circles indicate data-points for NGC 3311, colored according to the galactocentric distance. For other works, solid lines refer to local variations within galaxies (with a symbol indicating the center of the objects), and dashed lines refer to global variation across galaxies.

In the next sections, we try to understand what are the possible physical causes for the non-universality of the IMF in NGC 3311, as well as in other massive ETGs. To this purpose, we compare the results from NGC 3311 (obtained in B20, shown in all figures as data-points color-coded by distance from the center) with those obtained globally across different galaxies (dashed lines in all plots) and spatially within one or more objects (solid lines in all plots).

2.1. Correlations that do not hold for NGC 3311

The stellar velocity dispersion has been one of the first “drivers” proposed to explain the bottom-heaviness of the IMF both across different galaxies (van Dokkum & Conroy 2010; Treu et al. 2010; Conroy & van Dokkum 2012b; Cappellari et al. 2012; Spiniello et al. 2014) and within individual objects (Martín-Navarro et al. 2015a; Sarzi et al. 2018; La Barbera et al. 2019). However, recent indications have aroused questioning the IMF- σ_* relation, mainly based on the fact that the spatial gradients of the two quantities were often very different in radial extension (e.g. Sarzi et al. 2018). But, above all, the IMF slope has never been measured in galaxies with rising σ_* and $[\alpha/\text{Fe}]$ profiles like NGC 3311.

In the upper panel of Figure 1, we decidedly show that a direct linear correlation between the IMF bottom-heaviness and σ_* does not hold for NGC 3311. There, we compare the results of B20 with those obtained for M87 (red line, Sarzi et al. 2018), and from a sample of MaNGA (Bundy et al. 2015) galaxies, stacked in three mass bins (green lines, Parikh et al. 2018). We also show the global results obtained in La Barbera et al. (2013) based on a spectroscopic study on a large sample (~ 24000) of ETGs from the SPIDER Survey (La Barbera et al. 2009), performed with the same stellar population models (and the same IMF) used in B20. While a clear direct correlation is visible for all previous studies, a mild anti-correlation is inferred for NGC 3311, with the IMF slope being more bottom-heavy for points with lower σ_* . However, the IMF is dwarf-rich in the center of NGC 3311. As we will further show in the next section, all the results support a conjecture where the innermost region of massive galaxies is characterized by a dwarf-rich IMF, despite their kinematical properties.

Another parameter that has been reported to correlate directly with the IMF slope is the total metallicity ($[Z/H]$, Martín-Navarro et al. 2015c). Tentatively, a correlation can be seen for NGC 3311 in the lower panel of Figure 1, which is in agreement with the global results presented by the CALIFA Collaboration in Martín-Navarro et al. (2015c), and with the spatially resolved results obtained for M87 and the MaNGA stacked galaxies. These observational results suggest that the IMF is bottom-heavy for a more metal-rich population. Although we reproduce this relation, we also show that the slope of the correlation is almost perfectly aligned with the mean posterior distribution between the two parameters obtained in B20, shown as an ellipsoidal dashed line in the Figure. Therefore, there is strong ground to believe that the relation is at least partially due to an observational degeneracy between the two plotted quantities.²

Furthermore, from a theoretical perspective, simulations have demonstrated that the trends predicted by the IMF- $[Z/H]$ correlation fail to reproduce the general trend observed between the iron and α -element abundance (Gutcke & Springel 2019). Finally, we also note that other recent observational results (e.g., Martín-Navarro et al. 2019) indicate that the metallicity does not trace the IMF in spatially resolved observations³.

2.2. Correlations that do hold for NGC 3311

In Figure 2 we plot the observed relations between the IMF slope and radius (normalized by R_e , top panel), stellar age (middle panel) and surface stellar density (bottom panel). As in the previous figures, we compare the data points showing the results on NGC 3311 (obtained in B20) with lines showing the relations reported in the literature. Interestingly, these three plots support the following evidence: despite the different kinematical properties of the galaxies' central regions, the IMF is always dwarf-rich within the innermost few kilo-parsecs. There, according to the so-called two-phase formation scenario, the old and very dense “red-nugget” formed during the first phase of the mass assembly dominates the light.

² This evidence reinforces the importance of committing to a fully Bayesian approach and carefully inspecting the posterior probability results, not simply as a way to determine point estimates and uncertainties, but also as a tool to understand our limitations from an observational perspective.

³ The results in Martín-Navarro et al. (2019) suggest that, at least for the galaxy FCC 167, the metallicity track the distribution of cold orbits whereas the IMF slope that of warm orbits.

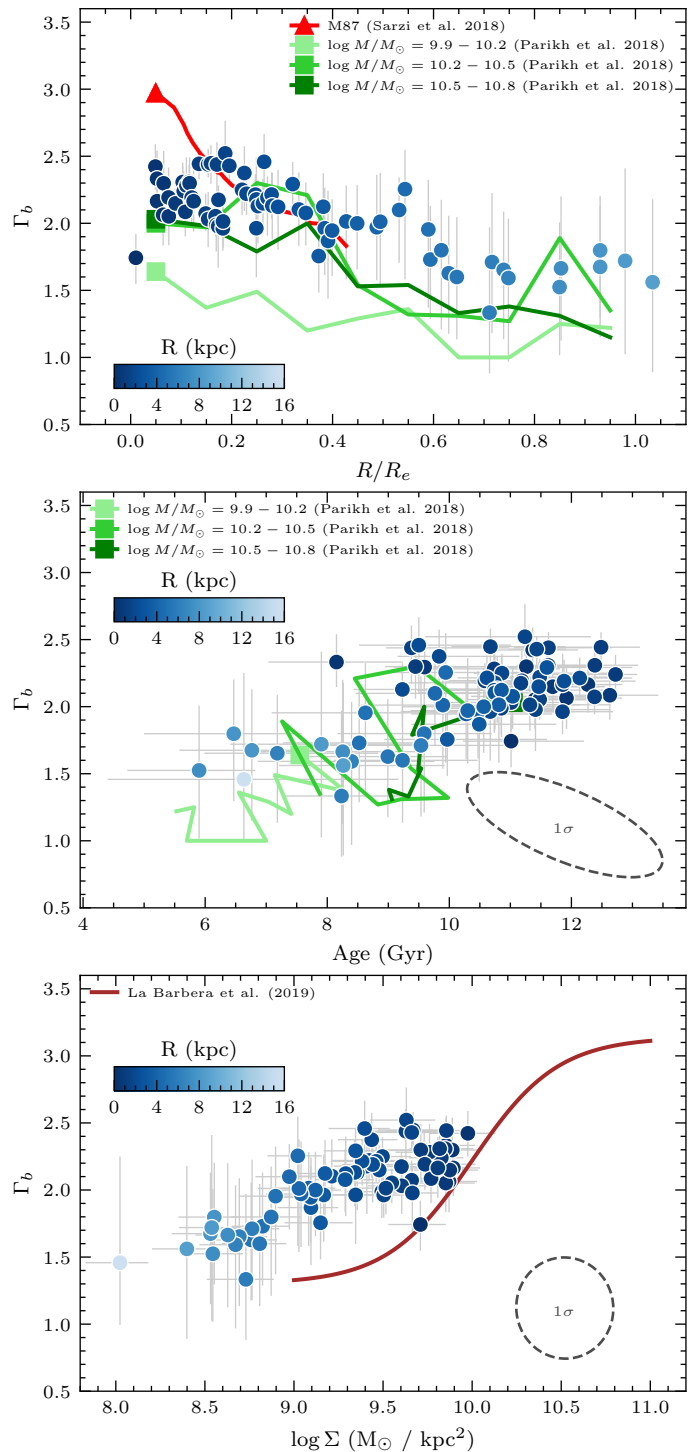


Fig. 2. The IMF spatial gradient (*upper panel*), and the correlation between Γ_b and the stellar age (*middle panel*) and between Γ_b and the total stellar density (*bottom panel*), all pointing towards the result that the IMF slope is bottom-heavy only for the “in situ” stars, formed at very high redshift from the first-phase of the two phase formation scenario.

In line with what has been suggested by other authors (van Dokkum et al. 2017; Martín-Navarro et al. 2019; Smith 2020), we, therefore, argue that the excess of dwarf stars may have originated from the first phase of galaxy formation in the early Universe, characterized by high density, temperature, and turbulence of the gas. These are, according to theoretical works (Hopkins 2012; Chabrier et al. 2014), key parameters driving the

fragmentation of molecular clouds (higher density and temperature should make the fragmentation easier, forming more dwarf stars, i.e. a bottom-heavier IMF)⁴. Later accretions of less massive satellites with an “MW-like” IMF (because formed later on, under less extreme temperature and density conditions), would settle preferentially in the galaxy periphery due to the lower densities and masses of the accreted systems and thus create spatial IMF gradient (Spavone et al. 2017; Pulsoni et al. 2020)⁵. Finally, our findings are consistent with those reported in Conroy & van Dokkum (2012b) and La Barbera et al. (2019), who found that the IMF becomes increasingly bottom-heavy when either the star formation timescale becomes shorter (see §2.3), or the surface density and/or the interstellar medium pressure increase.

2.3. The (apparently) puzzling case of the $[\alpha/\text{Fe}]$ abundance

According to the scenario described above, and in line with the results of B20, the central core of NGC 3311 is a “red-nugget” that formed its stars under extreme conditions. Such a short star formation time-scale would lead to a high $[\alpha/\text{Fe}]$ abundance (Thomas et al. 2005). This is explained by the fact that the star formation quenching took place before the Type Ia supernova explosions were able to pollute the interstellar medium with iron.

The α -abundance of stars in the innermost region of NGC 3311 is not extremely high (0.08 ± 0.02 , B20). In principle, this might question our conclusions that the stars in the core of NGC 3311 have been formed via a burst during the first phase of the two-phase scenario and with a dwarf-rich IMF. However, as showed in Fig 8 of B20, the NCG 3311 core requires a very large $[\text{Mg}/\text{Fe}]$ (> 0.3), which is, in practice, what was measured in Thomas et al. (2005), since they derived $[\alpha/\text{Fe}]$ from the absorption line indices Mgb and $\langle \text{Fe} \rangle$. The same is valid for the measurements performed in McDermid et al. (2014), which also proposed a direct global correlation between the IMF slope and the $[\alpha/\text{Fe}]$ but actually measured $[\text{Mg}/\text{Fe}]$ instead⁶. Hence, once again, the direct correlation found between the IMF slope and the $[\alpha/\text{Fe}]$ (or, more exactly, $[\text{Mg}/\text{Fe}]$) in other ETGs, e.g. M87, is found because for the majority of the massive ETGs the region where the $[\text{Mg}/\text{Fe}]$ is maximum spatially coincide with the region where the *in-situ* pristine population of stars dominates the light. We can now prove such a statement thanks to the unusual mass assembly of NGC 3311 (see B20 for more details), which caused an inverse α -element profile. In fact, in our case, Γ_b decreases when $[\alpha/\text{Fe}]$ increases, as shown in Figure 3. We stress that the offset between our results and those of Sarzi et al. (2018) and Parikh et al. (2018) is due to the fact that we measure variations in all the α -elements, rather than only Mg. The $[\text{Mg}/\text{Fe}]$ in the innermost region of NGC 3311 is indeed large (see Barbosa et al. 2018 and B20), thus these stars are compatible with having been formed via a burst of star formation. Finally, we note that the large $[\alpha/\text{Fe}]$ measured in the galactic halo of NGC 3311 is not caused by the fact that these stars have been formed at

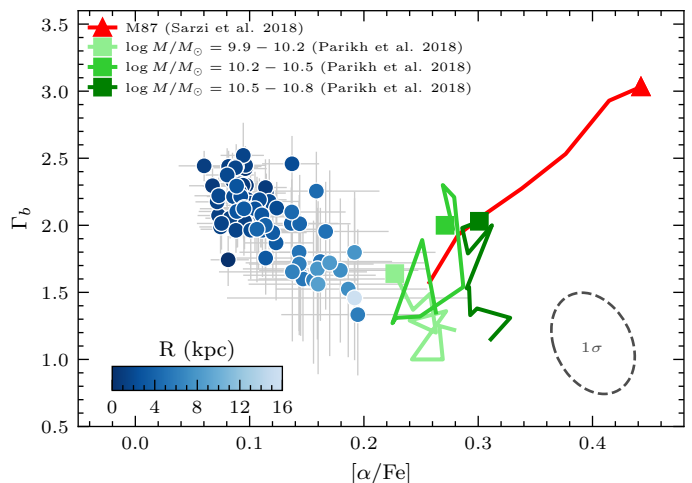


Fig. 3. IMF slope - $[\alpha/\text{Fe}]$ relation. For NGC 3311 (blue points) these two quantities are anti-correlated. This is the opposite of what happens for M87 (red). However, we stress that in B20 we used full-spectral fitting, rather than line-indices as in Sarzi et al. (2018) for M87, thus measuring a different quantity (from indices one is much more sensitive to Mg than to the “bulk” changes in all α elements). Note that the $[\alpha/\text{Fe}]$ estimates obtained in Barbosa et al. (2018) from the same data but using line-indices imply a high value, which would shift the blue data-points towards the red and green lines. The situation is much more complicated for the results based on MaNGA (green lines) where different galaxies, with possibly different $[\alpha/\text{Fe}]$ profiles are stacked together.

high- z “in situ” via a burst, but rather by the late accretion of previously quenched satellites (see B20 for more details).

In conclusion, all evidence points consistently to the fact that the IMF is dwarf-rich when stars are formed through a high- z intense and brief star formation episode.

3. Summary and Conclusion

In this letter, we used spatially resolved kinematical and stellar populations results from NGC 3311, the central galaxy of the Hydra I cluster to address the question of whether the relations between the low-mass end of the IMF slope and kinematical (σ_*) or stellar population (age, $[Z/\text{H}]$, $[\alpha/\text{Fe}]$) parameters are real, physically motivated relations. We find that the IMF- σ_* relation is mainly a spatial coincidence arising from the fact that the majority of massive ETGs show a σ_* profile that is peaked in the center likely because of violent relaxation (Hilz et al. 2012). This is not true for NGC 3311, but its core IMF is nonetheless bottom heavy. The strength of the IMF-metallicity direct correlation may instead be augmented by the degeneracy between Γ_b and $[Z/\text{H}]$, as addressed more extensively in the companion paper Barbosa et al. 2020.

We also presented our arguments in support of a two-phase formation scenario with two IMF with different low-mass end slope for the two distinct phases, as suggested by Smith (2020). This scenario is able to reconcile all the different observational and theoretical evidence in a spatially resolved sense, within a single galaxy, as well as in a “global” sense on large galaxy samples. Studying the IMF spatial gradients and the relation linking its slope Γ_b to the stellar age and that between Γ_b and stellar surface density, we explain the bottom-heaviness of the IMF as characteristics of the “relic” nucleus which was formed during the first phase, at very high- z in a violent, short, star formation episode ($\tau \sim 100\text{Myr}$, $\text{SFR} \geq 10^3 M_\odot \text{yr}^{-1}$). The accreted stellar component, which dominates the light budget at larger galacto-

⁴ Very recently a further parameter has been advocated by Davis & van de Voort (2020): the abundance of deuterium in the birth clouds of forming stars

⁵ In NGC 3311, the later mass accretion scenario is supported by the rising velocity dispersion profile that has been considered as the “smoking gun” of recent accretion of low-mass systems, dominating the dispersion scatter and leading to larger σ_* at larger distances (Hilker et al. 2018).

⁶ We refer the reader to B20 for more details about the different weight one gives to the α -elements when using line-index or when using full spectral fitting.

centric radii and was formed under less extreme and more time-extended star formation episodes (second phase), is instead described by a standard, “MW-like” IMF.

This version of the two-phase formation scenario naturally explains the radial IMF gradients recently reported for “normal” massive ETGs, but the very recent results obtained on “relic galaxies” provide further, independent support to this idea. Relics are rare local ultra-compact massive red and dead galaxies, which missed the second phase of accretion, thus evolving passively and unperturbed after the first burst of star formation. Since they missed this second phase, relics would have a bottom-heavy IMF everywhere, which is exactly what has been reported by Martín-Navarro et al. (2015b) and Ferré-Mateu et al. (2017) on the only three relics systems for which spatially resolved stellar population analysis has been performed so far. The outlook is bright, thanks to the newly started INSPIRE Project (Spiniello et al. 2020) which aims at confirming a larger number of relics at $z < 0.5$ and precisely infer their IMF slope thanks to high signal-to-noise ratio X-Shooter spectra.

Acknowledgements. The authors wish to acknowledge the anonymous referee for the constructive report. The authors acknowledge C. Mendes de Oliveira for discussions and suggestions. CEB gratefully acknowledges the São Paulo Research Foundation (FAPESP), grants 2011/51680-6, 2016/12331-0, 2018/24389-8. CS is supported by a Hintze Fellowship at the Oxford Centre for Astrophysical Surveys, which is funded through generous support from the Hintze Family Charitable Foundation. TR acknowledges support from the BASAL Centro de Astrofísica y Tecnologías Afines (CATA) PFB-06/2007.

This work is based on observations collected at the European Organisation for Astronomical Research in the Southern Hemisphere under ESO programme 094.B-0711(A). It has made use of the computing facilities of the Laboratory of Astroinformatics (Instituto de Astronomia, Geofísica e Ciências Atmosféricas, Departamento de Astronomia/USP, NAT/Unicisul), whose purchase was made possible by FAPESP (grant 2009/54006-4) and the INCT-A. This research has made use of the NASA/IPAC Extragalactic Database (NED), which is operated by the Jet Propulsion Laboratory, California Institute of Technology, under contract with the National Aeronautics and Space Administration.

References

- Barbosa, C. E., Arnaboldi, M., Coccato, L., et al. 2018, *A&A*, 609, A78
 Barbosa, C. E., Arnaboldi, M., Coccato, L., et al. 2016, *A&A*, 589, A139
 Brough, S., Proctor, R., Forbes, D. A., et al. 2007, *MNRAS*, 378, 1507
 Bundy, K., Bershady, M. A., Law, D. R., et al. 2015, *ApJ*, 798, 7
 Cappellari, M., McDermid, R. M., Alatalo, K., et al. 2012, *Nature*, 484, 485
 Carter, D., Bridges, T. J., & Hau, G. K. T. 1999, *MNRAS*, 307, 131
 Cenarro, A. J., Gorgas, J., Vazdekis, A., Cardiel, N., & Peletier, R. F. 2003, *MNRAS*, 339, L12
 Chabrier, G., Hennebelle, P., & Charlot, S. 2014, *ApJ*, 796, 75
 Conroy, C. & van Dokkum, P. 2012a, *ApJ*, 747, 69
 Conroy, C. & van Dokkum, P. G. 2012b, *ApJ*, 760, 71
 Davis, T. A. & van de Voort, F. 2020, *MNRAS*, 498, 4051
 Emsellem, E., Krajnovic, D., & Sarzi, M. 2014, *MNRAS*, 445, L79
 Ferré-Mateu, A., Trujillo, I., Martín-Navarro, I., et al. 2017, *MNRAS*, 467, 1929
 Fisher, D., Illingworth, G., & Franx, M. 1995, *ApJ*, 438, 539
 Gutcke, T. A. & Springel, V. 2019, *MNRAS*, 482, 118
 Hilker, M., Richtler, T., Barbosa, C. E., et al. 2018, *A&A*, 619, A70
 Hilz, M., Naab, T., Ostriker, J. P., et al. 2012, *MNRAS*, 425, 3119
 Hopkins, P. F. 2012, *MNRAS*, 423, 2037
 La Barbera, F., de Carvalho, R. R., de la Rosa, I. G., et al. 2009, *arXiv e-prints*, arXiv:0912.4547
 La Barbera, F., Ferreras, I., Vazdekis, A., et al. 2013, *MNRAS*, 433, 3017
 La Barbera, F., Vazdekis, A., Ferreras, I., et al. 2019, *MNRAS*, 489, 4090
 La Barbera, F., Vazdekis, A., Ferreras, I., et al. 2017, *MNRAS*, 464, 3597
 Martín-Navarro, I., La Barbera, F., Vazdekis, A., Falcón-Barroso, J., & Ferreras, I. 2015a, *MNRAS*, 447, 1033
 Martín-Navarro, I., La Barbera, F., Vazdekis, A., et al. 2015b, *MNRAS*, 451, 1081
 Martín-Navarro, I., Lyubenova, M., van de Ven, G., et al. 2019, *A&A*, 626, A124
 Martín-Navarro, I., Vazdekis, A., La Barbera, F., et al. 2015c, *ApJ*, 806, L31
 McDermid, R. M., Cappellari, M., Alatalo, K., et al. 2014, *ApJ*, 792, L37
 Naab, T., Johansson, P. H., & Ostriker, J. P. 2009, *ApJ*, 699, L178
 Oser, L., Ostriker, J. P., Naab, T., Johansson, P. H., & Burkert, A. 2010, *ApJ*, 725, 2312
 Parikh, T., Thomas, D., Maraston, C., et al. 2018, *MNRAS*, 477, 3954
 Pulsoni, C., Gerhard, O., Arnaboldi, M., et al. 2020, *arXiv e-prints*, arXiv:2009.01823
 Rodriguez-Gomez, V., Pillepich, A., Sales, L. V., et al. 2016, *MNRAS*, 458, 2371
 Sarzi, M., Spiniello, C., La Barbera, F., Krajnovic, D., & van den Bosch, R. 2018, *MNRAS*, 478, 4084
 Sembach, K. R. & Tonry, J. L. 1996, *AJ*, 112, 797
 Smith, R. J. 2020, *ARA&A*, 58, 577
 Spavone, M., Capaccioli, M., Napolitano, N. R., et al. 2017, *A&A*, 603, A38
 Spiniello, C., Barnabè, M., Koopmans, L. V. E., & Trager, S. C. 2015, *MNRAS*, 452, L21
 Spiniello, C., Tortora, C., D’Ago, G., et al. 2020, *arXiv e-prints*, arXiv:2011.05347
 Spiniello, C., Trager, S., Koopmans, L. V. E., & Conroy, C. 2014, *MNRAS*, 438, 1483
 Spiniello, C., Trager, S. C., Koopmans, L. V. E., & Chen, Y. P. 2012, *ApJ*, 753, L32
 Thomas, D., Maraston, C., Bender, R., & Mendes de Oliveira, C. 2005, *ApJ*, 621, 673
 Treu, T., Auger, M. W., Koopmans, L. V. E., et al. 2010, *ApJ*, 709, 1195
 van Dokkum, P., Conroy, C., Villaume, A., Brodie, J., & Romanowsky, A. J. 2017, *ApJ*, 841, 68
 van Dokkum, P. G. & Conroy, C. 2010, *Nature*, 468, 940
 Vaughan, S. P., Davies, R. L., Zieleniewski, S., & Houghton, R. C. W. 2018, *MNRAS*, 479, 2443
 Vazdekis, A., Casuso, E., Peletier, R. F., & Beckman, J. E. 1996, *ApJS*, 106, 307
 Vazdekis, A., Koleva, M., Ricciardelli, E., Röck, B., & Falcón-Barroso, J. 2016, *MNRAS*, 463, 3409
 Veale, M., Ma, C.-P., Thomas, J., et al. 2017, *MNRAS*, 464, 356